

Performance of mMIMO FD Relay Networks with Limited Relay State Knowledge

Original

Performance of mMIMO FD Relay Networks with Limited Relay State Knowledge / Nordio, A., Chiasserini, C.F.. - In: IEEE WIRELESS COMMUNICATIONS LETTERS. - ISSN 2162-2337. - STAMPA. - 11:5(2022), pp. 1032-1036. [10.1109/LWC.2022.3153798]

Availability:

This version is available at: 11583/2955885 since: 2022-05-11T10:32:06Z

Publisher:

IEEE

Published

DOI:10.1109/LWC.2022.3153798

Terms of use:

This article is made available under terms and conditions as specified in the corresponding bibliographic description in the repository

Publisher copyright

IEEE postprint/Author's Accepted Manuscript

©2022 IEEE. Personal use of this material is permitted. Permission from IEEE must be obtained for all other uses, in any current or future media, including reprinting/republishing this material for advertising or promotional purposes, creating new collecting works, for resale or lists, or reuse of any copyrighted component of this work in other works.

(Article begins on next page)

Performance of mMIMO FD Relay Networks with Limited Relay State Knowledge

Alessandro Nordinio, *Member, IEEE*, Carla Fabiana Chiasserini, *Fellow, IEEE*

Abstract—Massive MIMO (mMIMO) is a key technology for improving propagation conditions and extending geographical coverage of wireless communications. We here address a mMIMO full-duplex relay network for machine-type-communications where channel state information availability at the transmitter is impractical. In this scenario, we argue that high end-to-end data rates can be achieved even if no precoding is performed at the transmitting nodes. We first formulate an optimization problem aiming at maximizing the achievable rate, considering the source transmit power to depend on the transmit power distribution at the relay node. We then solve this problem by letting the number of antennas grow large, and derive closed-form expressions for the transmit power at the source and relay, as well as for the system data rate. Our results, show that the rate obtained when no precoding is implemented at the relay, or at any of the transmitters, closely matches that of SVD precoding under the optimum receiver, and still achieves very high values in the case of the ZF and the MMSE receiver.

Index Terms—mMIMO, Relay networks, Achievable rate

I. INTRODUCTION

Massive multiple-input-multiple-output (mMIMO) communication is one of the key technologies in 5G/6G, as, thanks to the large number of spatial degrees of freedom (DoF), it makes channel conditions appear almost constant over time and allows for better propagation. In spite of such benefits, which can greatly improve the capacity and geographical coverage of communication systems, mMIMO connectivity for machine-type-communications (MTC) is still in infancy [1], [2]. Indeed, a high number of spatial DoFs can be achieved only through an accurate estimation of channel state information (CSI), which, due to the large number of antennas used for mMIMO, can be very time and bandwidth consuming. Additionally, MTC scenarios include numerous devices, but only few are active at a given point in time, and detecting (and estimating the channel for) the communication links to be used is highly challenging. These factors combined together make availability of CSI at the transmitter in mMIMO MTC hard to achieve.

Prior work on mMIMO in MTC single-hop networks can be found in, e.g., [3], which presents a channel approximation model and a channel estimation algorithm. In an amplify-and-forward relay network, [4], [5] determine, respectively, the power allocation and the pilot length maximizing the system performance. mMIMO relay networks are instead addressed in [6], where two transmission protocols for single-antenna users are studied, and [7] where however all transmitters have perfect CSI knowledge and, hence, apply precoding.

In this paper, we take a different perspective from previous work and argue that, when CSI knowledge at the transmitter is lacking and a sufficiently accurate estimation thereof is impractical, it may be more beneficial not to perform precoding.

Specifically, unlike prior art, we tackle a mMIMO full-duplex (FD) relay network working in decode-and-forward (DF) mode and where the destination is an MTC device, and optimize the transmit power at the source (e.g., a cellular base station) and relay, so as to maximize the achievable rate in absence of precoding. We consider both the case where precoding is implemented at neither the source nor the relay, which reflects the case where the relay is a capability-constrained device, and that where only the source performs precoding, which corresponds to the case where the relay is able to send appropriate feedback to the source. Further, we consider that different receivers, namely, optimal, zero-forcing (ZF), and minimum mean square error (MMSE), can be used. In these scenarios, we provide the following main contributions:

(i) We argue that no-precoding at the transmitters in mMIMO FD relay networks can lead to excellent performance, when the values of transmit power are optimally selected. To support our claim, we formulate the problem of maximizing the achievable rate in such networks, accounting for all main system constraints and making the source transmit power depend on the transmit power distribution at the relay;

(ii) In light of the problem complexity, we first optimize the source transmit power to maximize the rate on the source-destination link, given the relay transmit power distribution;

(iii) We then consider that the number of antennas at the network nodes grows large while their ratios remain constant, and present an asymptotic analysis of the system rate that provides a closed-form expression for the transmitters' power as well as for the system achievable rate;

(iv) Through numerical analysis, we show the excellent performance that can be obtained when compared to the case where SDV precoding is implemented.

We remark that, to our knowledge, we are the first to provide such analysis and to show the performance of different approaches for rate maximization in mMIMO FD relay networks with no precoding.

The rest of the paper is organized as follows. Sec. II introduces our system model and achievable rate maximization in an mMIMO FD relay network. Sec. III discusses how to determine the source transmit power, while our asymptotic analysis and closed-form expressions for the transmit power and data rate are derived in Sec. IV. Finally, Sec. V compares the performance of our scheme against the case where SVD precoding is implemented, and Sec. VI concludes the paper.

II. ACHIEVABLE RATE MAXIMIZATION IN mMIMO FULL-DUPLEX RELAY NETWORKS

In this section, we first describe the system model considering a finite number of antennas at the network nodes.

Then, given such a scenario, we formulate the problem of maximizing the system achievable rate.

A. System Model

We consider a 2-hop wireless relay network (although the results apply to 1-hop networks as well), as depicted in Fig. 1, where data source \mathcal{S} , i.e., a cellular base station, cannot directly communicate with destination \mathcal{D} , i.e., a MTC device. Connectivity between \mathcal{S} and \mathcal{D} is permitted by relay node \mathcal{R} , which can operate in FD mode. \mathcal{R} decodes the message sent by \mathcal{S} and re-encodes it on the $\mathcal{R}-\mathcal{D}$ link (DF); in the following, variables with subscript $i=1,2$ refer to the first ($\mathcal{S}-\mathcal{R}$) and the second ($\mathcal{R}-\mathcal{D}$) link, respectively.

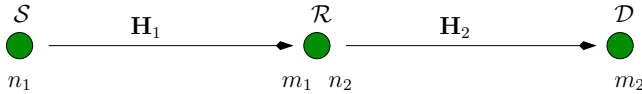


Fig. 1. Full-duplex relay network scenario.

We also assume that all network nodes are equipped with multiple antennas, namely, \mathcal{S} has n_1 transmit antennas, \mathcal{R} has n_2 and m_1 transmit and receive antennas, respectively, while \mathcal{D} has m_2 antennas. Receivers of both links have perfect CSI; on the contrary, CSI is not available at the transmitters, e.g., the relay has knowledge of the $\mathcal{S}-\mathcal{R}$ channel, but it does not have knowledge of the $\mathcal{R}-\mathcal{D}$ channel.

Next, consider a period of time where both channels are static and where both source and relay transmit with power $p_1 \in [0, p_1^{\max}]$ and $p_2 \in [0, p_2^{\max}]$, respectively. Then the signal at the receiver of the i -th link can be described by the vector

$$\mathbf{y}_i = \sqrt{p_i \alpha_i} \mathbf{H}_i \mathbf{x}_i + \boldsymbol{\eta}_i \quad (1)$$

where \mathbf{x}_i is the vector of transmitted random symbols. We assume \mathbf{x}_i to be a Gaussian complex multivariate random variable with zero mean and covariance $\mathbb{E}[\mathbf{x}_i \mathbf{x}_i^H] = \frac{1}{n_i} \mathbf{I}$. The coefficient α_i is the path loss and the $m_i \times n_i$ matrix \mathbf{H}_i contains the channel coefficients of the i -th link. The vector $\boldsymbol{\eta}_i$ accounts for the thermal noise, for any possible interference affecting the reception, and, in the case of the $\mathcal{S}-\mathcal{R}$ link, also for the self-interference. It is modeled as a complex Gaussian multivariate random variable with independent and identically distributed (iid) entries, zero mean and covariance $\mathbb{E}[\boldsymbol{\eta}_i \boldsymbol{\eta}_i^H] = N_i \mathbf{I}$. This is in accordance with prior work [7]–[9] that assumes the self-interference power to be proportional to the relay average transmit power p_2 , through the coefficient β , which accounts for analog and digital attenuation techniques implemented at the relay. Thus, we write $N_1 = I_1 + \beta p_2$ where I_1 represents the contribution of the thermal noise. Since the $\mathcal{R}-\mathcal{D}$ link does not suffer from self-interference, we write $N_2 = I_2$. Note that the term $\boldsymbol{\eta}_1$ on the $\mathcal{S}-\mathcal{R}$ link is independent of \mathbf{x}_1 , as it depends upon the information previously sent by \mathcal{S} , and currently relayed by \mathcal{R} , but not on the information that \mathcal{S} is currently transmitting.

B. Receiver models and achievable link rates

To decode the transmitted data, the receiver has several options. The optimum receiver can jointly decode all symbols

in \mathbf{x}_i , thus achieving rate

$$\rho_i = \log_2 \left| \mathbf{I} + p_i s_i \tilde{\mathbf{H}}_i^H \tilde{\mathbf{H}}_i \right| = \sum_{j=1}^{n_i} \log_2 (1 + p_i s_i \lambda_{i,j}) \quad (2)$$

where $\tilde{\mathbf{H}}_i = \frac{\mathbf{H}_i}{\sqrt{m_i}}$, $s_i = \frac{\alpha_i m_i}{N_i n_i}$, and $\lambda_{i,j}$ is the j -th eigenvalue of $\tilde{\mathbf{H}}_i^H \tilde{\mathbf{H}}_i$. As an alternative, simpler suboptimal linear receivers can be used. Such receivers first multiply \mathbf{y}_i by an $n_i \times m_i$ filter, \mathbf{B}_i , forming the vectors

$$\mathbf{z}_i = \mathbf{B}_i \mathbf{y}_i, \quad i = \{1, 2\} \quad (3)$$

and then separately decode the symbols in \mathbf{x}_i by using the corresponding elements in \mathbf{z}_i . Several choices for matrix \mathbf{B}_i are possible. In this work, we consider the following cases:

- the zero-forcing (ZF) receiver where $\mathbf{B}_i = (\tilde{\mathbf{H}}_i^H \tilde{\mathbf{H}}_i)^{-1} \tilde{\mathbf{H}}_i^H$ and
- the minimum mean square error (MMSE) receiver where $\mathbf{B}_i = (\mathbf{I} + p_i s_i \tilde{\mathbf{H}}_i^H \tilde{\mathbf{H}}_i)^{-1} \tilde{\mathbf{H}}_i^H$.

Then, under such receivers, the achievable rate on the i -th link can be compactly written as

$$\rho_i = \sum_{j=1}^{n_i} \log (1 + w_{i,j}) \quad \text{where} \quad (4)$$

$$w_{i,j} = \begin{cases} p_i s_i \lambda_{i,j} & \text{for the optimum receiver} \\ \frac{p_i s_i}{[(\tilde{\mathbf{H}}_i^H \tilde{\mathbf{H}}_i)^{-1}]_{j,j}} & \text{for the ZF receiver} \\ \frac{1}{[(\mathbf{I} + p_i s_i \tilde{\mathbf{H}}_i^H \tilde{\mathbf{H}}_i)^{-1}]_{j,j}} - 1 & \text{for the MMSE receiver} \end{cases} \quad (5)$$

Notice that rate ρ_1 is a function of both p_1 and p_2 , since the latter appears in the expression of N_1 , which, in turns, contributes to s_1 . Instead, ρ_2 is a function of the transmitted power p_2 only. Thus, in the following we denote these rates by $\rho_1(p_1, p_2)$ and $\rho_2(p_2)$, respectively. Communication between \mathcal{S} and \mathcal{D} takes place over a sequence of time slots, each one characterized by specific values of source and relay transmit power. Let $g(p_2)$, $p_2 \in [0, p_2^{\max}]$, be the distribution of the relay transmit power p_2 . Then the average rates achieved on the $\mathcal{S}-\mathcal{R}$ and $\mathcal{R}-\mathcal{D}$ links are, respectively, given by

$$R_1(g, p_1) = \int_0^{p_2^{\max}} g(p_2) \rho_1(p_1, p_2) dp_2; \quad R_2(g) = \int_0^{p_2^{\max}} g(p_2) \rho_2(p_2) dp_2 \quad (6)$$

where p_2^{\max} is the maximum transmit power the relay can use on a single slot, and, by writing $R_1(g, p_1)$ and $R_2(g)$, we stress the fact that such average rates depend on the specific choice of distribution $g(\cdot)$. The source transmit power, p_1 , can be optimized, depending on the relay transmit power, p_2 . It follows that p_1 can be thought as a function, $p_1(p_2)$, of the relay transmit power p_2 . At last, we assume that the average transmit power at both source and relay is set to \bar{p}_1 and \bar{p}_2 , respectively. In other words, we impose:

$$(a) \int_0^{p_2^{\max}} p_2 g(p_2) dp_2 = \bar{p}_2; \quad (b) \int_0^{p_2^{\max}} p_1(p_2) g(p_2) dp_2 = \bar{p}_1. \quad (7)$$

C. Problem statement

We are interested in finding the maximum end-to-end rate, R , achievable between \mathcal{S} and \mathcal{D} . To this end, we formulate the following optimization problem:

$$\begin{aligned} \mathbf{P0}: R &= \max_{g(\cdot), p_1(\cdot)} \min \{R_1(g, p_1), R_2(g)\} \\ &= \max_{g(\cdot)} \min_{p_1(\cdot)} \left\{ \max_{p_1(\cdot)} R_1(g, p_1), R_2(g) \right\} \end{aligned} \quad (8)$$

subject to (7) and $\int_0^{p_2^{\max}} g(p_2) dp_2 = 1, g(p_2) \geq 0$. As shown in [7], the maximizing distribution is typically discrete and composed of few isolated probability masses in $[0, p_2^{\max}]$.

III. SOURCE TRANSMIT POWER OPTIMIZATION

The first step towards the solution of **P0** is to optimize rate $R_1(g, p_1)$ for $p_1 \in [0, p_1^{\max}]$, for any given $g(\cdot)$ such that it meets constraint (7)a, under the constraint (7)b. To do so, we define the Lagrangian

$$\mathcal{L}(p_1, p_2) = g(p_2)\rho_1(p_1, p_2) - n_1\psi p_1 g(p_2)$$

where ψ is a Lagrange multiplier and we solve for p_1^* the equation $\frac{\partial}{\partial p_1^*} \mathcal{L}(p_1^*, p_2) = 0$. By using (4), we obtain

$$\psi = \frac{1}{n_1} \frac{d}{dp_1^*} \rho_1(p_1^*, p_2) = \frac{1}{n_1} \sum_{j=1}^{n_1} \frac{\frac{d}{dp_1^*} w_{1,j}}{1 + w_{1,j}} \quad (9)$$

which holds for $p_1^* \in [0, p_1^{\max}]$. In (9), $p_1^* = p_1^*(p_2)$ is the optimal power profile at \mathcal{S} , which depends on the transmit power at \mathcal{R} . Note that $p_1^*(p_2)$ also depends on the multiplier ψ that has to satisfy (7)b, where $p_1(p_2)$ is to be replaced with $p_1^*(p_2)$.

Using quantities $w_{i,j}$ in (5), we specialize (9) as follows:

$$\psi = \frac{1}{n_1} \sum_{j=1}^{n_1} \frac{s_1 \lambda_{1,j}}{1 + p_1^* s_1 \lambda_{1,j}} \quad (10)$$

for the optimum receiver and

$$\psi = \frac{1}{n_1} \sum_{j=1}^{n_1} \frac{s_1}{[(\tilde{\mathbf{H}}_1^H \tilde{\mathbf{H}}_1)^{-1}]_{j,j} + p_1^* s_1} \quad (11)$$

for the ZF receiver. As for the MMSE receiver, we first define $\mathbf{W} = \mathbf{I} + p_1^* s_1 \tilde{\mathbf{H}}_1^H \tilde{\mathbf{H}}_1$ and we get

$$\begin{aligned} \psi &= \frac{1}{n_1} \sum_{j=1}^{n_1} \frac{\frac{\partial}{\partial p_1^*} \left(\frac{1}{[\mathbf{W}^{-1}]_{j,j}} - 1 \right)}{1 + \frac{1}{[\mathbf{W}^{-1}]_{j,j}} - 1} \\ &= \frac{s_1}{n_1} \sum_{j=1}^{n_1} \frac{[\mathbf{W}^{-1} \tilde{\mathbf{H}}_1^H \tilde{\mathbf{H}}_1 \mathbf{W}^{-1}]_{j,j}}{[\mathbf{W}^{-1}]_{j,j}} \end{aligned} \quad (12)$$

Observe that the expressions in (10), (11) and (12) are difficult to solve for p_1^* and, thus, a closed-form expression for $p_1^*(p_2)$ is not available in general, as it would require to solve a polynomial expression with degree equal to n_i . Nonetheless, some general considerations can be made. First, it is easy to see that $\frac{d}{dp_2} p_1^*(p_2) \leq 0$, i.e., $p_1^*(p_2)$ is a non-increasing function of p_2 . Hence, a unique real solution for $p_1^*(p_2)$ of (9) exists. This can be proved by observing that $\frac{d}{dp_2} p_1^*(p_2) = -\frac{\partial t(p_1^*, p_2)/\partial p_2}{\partial t(p_1^*, p_2)/\partial p_1^*}$ is

negative, where $t(p_1^*, p_2) = \frac{1}{n_1} \frac{d}{dp_1^*} \rho_1(p_1^*, p_2)$ is the implicit function in (9).

As $N_1 \rightarrow 0$, we have $s_1 \rightarrow \infty$ and, hence, $p_1^* \rightarrow \frac{1}{\psi}$ for all considered receive filters. This result can be obtained by taking the limit for $s_1 \rightarrow \infty$ of the r.h.s of (10), (11) and (12) (for the optimum receiver, we assume a full-rank matrix $\tilde{\mathbf{H}}_1^H \tilde{\mathbf{H}}_1$). Also, taking the limit for $p_1^* \rightarrow 0$ in (10), we obtain $\psi = s_1 \bar{\lambda}_1$, i.e., $p_2 = \frac{1}{\beta} \left(\frac{\alpha_1 m_1}{\psi n_1} \bar{\lambda}_1 - I_1 \right) \triangleq \omega^{\text{OPT}}$, where $\bar{\lambda}_1 = \frac{1}{n_1} \sum_{j=1}^{n_1} \lambda_{1,j}$ is the average eigenvalue of $\tilde{\mathbf{H}}_1^H \tilde{\mathbf{H}}_1$. The same expression is obtained by taking the limit for $p_1^* \rightarrow 0$ of (12). Indeed, one can observe that the average eigenvalue $\bar{\lambda}_1$, can also be written as $\bar{\lambda}_1 = \frac{1}{n_1} \sum_{j=1}^{n_1} [(\tilde{\mathbf{H}}_1^H \tilde{\mathbf{H}}_1)_{j,j}]$. Instead, the limit applied to (11) provides $\psi = \frac{s_1}{n_1} \sum_{j=1}^{n_1} \frac{1}{[(\tilde{\mathbf{H}}_1^H \tilde{\mathbf{H}}_1)^{-1}]_{j,j}}$, i.e., $p_2 = \frac{1}{\beta} \left(\frac{\alpha_1 m_1}{\psi n_1^2} \sum_{j=1}^{n_1} \frac{1}{[(\tilde{\mathbf{H}}_1^H \tilde{\mathbf{H}}_1)^{-1}]_{j,j}} - I_1 \right) \triangleq \omega^{\text{ZF}}$. Since $p_1^*(p_2)$ is non-negative (being a power), from the above considerations it follows that $p_1^*(p_2) = 0$ for $p_2 > \omega^{\text{OPT}}$ (OPT and MMSE receivers), and for $p_2 > \omega^{\text{ZF}}$ (ZF receiver).

In the next section, we show instead that, when the number of antennas at the network nodes grows large (while keeping their ratios constant), we can obtain a closed-form expression for the transmit power at source and relay, as well as for the system end-to-end achievable rate.

IV. MMIMO: ASYMPTOTIC ANALYSIS

We now consider the case where the number of antennas at \mathcal{S} , \mathcal{R} , and \mathcal{D} grows large, while their ratios $\frac{n_1}{m_1} = \zeta_1$, $\frac{n_2}{m_2} = \zeta_2$, and $\frac{m_1}{n_2} = \zeta_r$ remain constant. In such a case, it is more appropriate to consider as performance metric the *normalized* rate R/n_1 (i.e., the rate per source transmit antenna), instead of R . Also, in order to keep a lighter notation, we will use the symbol \lim to denote the limit $\lim_{n_1, m_1, n_2, m_2 \rightarrow \infty}$ under the constraint of constant ratios ζ_1 , ζ_2 , and ζ_r . Then, by using (8), we define the asymptotic normalized rate:

$$R^\infty \triangleq \lim_{n_1} \frac{R}{n_1} = \max_{g(\cdot)} \min \left\{ R_1^{*,\infty}(g), \frac{\zeta_r}{\zeta_1} R_2^\infty(g) \right\} \quad (13)$$

$R_1^{*,\infty}(g)$ and $R_2^\infty(g)$ are the asymptotic normalized rates on $\mathcal{S}-\mathcal{R}$ and $\mathcal{R}-\mathcal{D}$, respectively,

$$R_1^{*,\infty}(g) \triangleq \lim_{n_1} \frac{R_1^*(g)}{n_1} = \int_0^{p_2^{\max}} g(p_2) \lim_{n_1} \frac{\rho_1^*(p_2)}{n_1} dp_2 \quad (14)$$

$$R_2^\infty(g) \triangleq \lim_{m_2} \frac{R_2(g)}{m_2} = \int_0^{p_2^{\max}} g(p_2) \lim_{m_2} \frac{\rho_2(p_2)}{n_2} dp_2 \quad (15)$$

In the asymptotic regime, the eigenvalues of matrices \mathbf{H}_1 and \mathbf{H}_2 assume particular properties. More specifically, if \mathbf{H}_j , $j = 1, 2$ is an instance of matrix-variate random variable whose entries are i.i.d., have zero-mean and variance 1, then, as its size grows to infinity with constant ratio $\zeta_j \geq 1$, the distribution of the generic eigenvalue λ of $\frac{1}{m_j} \mathbf{H}_j^H \mathbf{H}_j$ tends to the Marčenko-Pastur law [7]: $f_j(\lambda) = \frac{\sqrt{(\lambda - a_j)(b_j - \lambda)}}{2\pi \lambda \zeta_j}$ with support in $[a_j, b_j]$, where $a_j = (1 - \sqrt{\zeta_j})^2$, $b_j = (1 + \sqrt{\zeta_j})^2$, and $j = 1, 2$. Also, the average eigenvalue is

given by $\bar{\lambda}_j = 1$. Given the above asymptotic eigenvalue distribution, for convenience we define

$$\begin{aligned} G(\gamma, \zeta_j) &\triangleq \int_{a_j}^{b_j} \log(1 + \gamma\lambda) f_j(\lambda) d\lambda \\ &= \log\left(1 + \gamma - \frac{F(\gamma, \zeta_j)}{4}\right) - \frac{F(\gamma, \zeta_j)}{4\zeta_j\gamma} \\ &\quad + \frac{1}{\zeta_j} \log\left(1 + \gamma\zeta_j - \frac{F(\gamma, \zeta_j)}{4}\right) \end{aligned} \quad (16)$$

where $F(\gamma, \zeta_j) \triangleq (\sqrt{\gamma b_j + 1} - \sqrt{\gamma a_j + 1})^2$.

Optimum receiver. In the asymptotic mMIMO regime, the optimal source power, $p_1^*(p_2)$, tends to the asymptotic power $p_1^{*,\infty}(p_2)$ whose expression can be explicitly derived from (9). Indeed, $\psi^\infty \triangleq \lim \psi$ is given by:

$$\psi^\infty = \lim \frac{1}{n_1} \sum_{j=1}^{n_1} \frac{s_1 \lambda_{1,j}}{1 + p_1^* s_1 \lambda_{1,j}} = \frac{s_1}{4\zeta_1} \frac{F(p_1^{*,\infty} s_1, \zeta_1)}{(p_1^{*,\infty} s_1)^2} \quad (17)$$

The above equation has two solutions for $p_1^{*,\infty}$; however, recalling that $p_1^{*,\infty}(p_2)$ must be a decreasing function of p_2 and that $p_1^{*,\infty} \in [0, p_1^{\max}]$, we obtain:

$$p_1^{*,\infty} = \min \left\{ p_1^{\max}, \left[\frac{1 + \zeta_1 - \sqrt{(1 - \zeta_1)^2 + 4\zeta_1 \psi^\infty / s_1}}{2\psi^\infty \zeta_1} \right]^+ \right\}$$

From the discussion in Sec. III, we also find that $p_1^{*,\infty} > 0$ for $p_2 < \omega^{\text{OPT}} = \frac{1}{\beta} \left(\frac{\alpha_1}{\psi^\infty \zeta_1} - I_1 \right)$. In the asymptotic regime, the normalized rate achieved on the $\mathcal{S}-\mathcal{R}$ link is given by

$$\begin{aligned} \rho_1^{*,\infty}(p_2) &= \lim \frac{\rho_1^*(p_2)}{n_1} \\ &= \lim \frac{1}{n_1} \sum_{j=1}^{n_1} \log(1 + p_1^* s_1 \lambda_{1,j}) = G(\gamma_1, \zeta_1) \end{aligned} \quad (18)$$

where we defined $\gamma_1 \triangleq p_1^{*,\infty} s_1$. Similarly, defining $\gamma_2 \triangleq \frac{p_2 \alpha_2}{\zeta_2 I_2}$, the normalized $\mathcal{R}-\mathcal{D}$ rate is given by:

$$\rho_2^\infty(p_2) = \lim \frac{\rho_2(p_2)}{n_2} = G(\gamma_2, \zeta_1) \quad (19)$$

ZF receiver. If the ZF filter is employed at the relay receiver, the asymptotic optimal power profile can be obtained by taking the limit of (11). For $p_1^* \in [0, p_1^{\max}]$, we get

$$\psi^\infty = \lim \frac{1}{n_1} \sum_{j=1}^{n_1} \frac{s_1}{[(\tilde{\mathbf{H}}_1^H \tilde{\mathbf{H}}_1)^{-1}]_{j,j} + p_1^* s_1} = \frac{s_1}{\frac{1}{1 - \zeta_1} + p_1^{*,\infty} s_1}$$

since $[(\tilde{\mathbf{H}}_1^H \tilde{\mathbf{H}}_1)^{-1}]_{j,j} \rightarrow \frac{1}{1 - \zeta_1} \forall j$. It follows that:

$$p_1^{*,\infty} = \min \left\{ p_1^{\max}, \left[\frac{1}{\psi^\infty} - \frac{1}{s_1(1 - \zeta_1)} \right]^+ \right\},$$

$p_1^{*,\infty} > 0$ for $p_2 < \omega^{\text{ZF}} = \frac{1}{\beta} \left(\frac{\alpha_1(1 - \zeta_1)}{\psi^\infty \zeta_1} - I_1 \right)$ and

$$\rho_1^\infty(p_2) = \lim \frac{1}{n_1} \sum_{j=1}^{n_1} \log \left(1 + \frac{p_1^* s_1}{[(\mathbf{H}_1^H \mathbf{H}_1)^{-1}]_{j,j}} \right) = \log \frac{s_1(1 - \zeta_1)}{\psi^\infty}$$

$$\begin{aligned} \rho_2^\infty(p_2) &= \lim \frac{1}{n_2} \sum_{j=1}^{n_2} \log \left(1 + \frac{p_2 s_2}{[(\mathbf{H}_2^H \mathbf{H}_2)^{-1}]_{j,j}} \right) \\ &= \log(1 + p_2 s_2 (1 - \zeta_2)) \end{aligned} \quad (20)$$

MMSE receiver. As for the MMSE receiver, we first observe that for any j , $\lim [\mathbf{W}^{-1}]_{j,j} = \frac{1}{1 + \gamma_1 - F(\gamma_1, \zeta_1)/4}$ where we recall that $\mathbf{W} = \mathbf{I} + \gamma_1 \tilde{\mathbf{H}}_1^H \tilde{\mathbf{H}}_1$ and $\gamma_1 = p_1^{*,\infty} s_1$. Thus, following (12), we can write:

$$\begin{aligned} \psi^\infty &= \lim \frac{1}{n_1} \sum_{j=1}^{n_1} [\mathbf{W}^{-1}]_{j,j} \frac{\partial}{\partial p_1^*} \left(\frac{1}{[\mathbf{W}^{-1}]_{j,j}} \right) \\ &= \frac{s_1}{4(1 + \gamma_1) - F(\gamma_1, \zeta_1)} \left(4 - \frac{\partial F(\gamma_1, \zeta_1)}{\partial \gamma_1} \right) \end{aligned} \quad (21)$$

The above expression can be solved numerically for $p_1^{*,\infty} \in [0, p_1^{\max}]$. Furthermore,

$$\rho_1^{*,\infty}(p_2) = \lim \frac{-\sum_{j=1}^{n_1} \log[\mathbf{W}^{-1}]_{j,j}}{n_1} = \log \left(1 + \gamma_1 - \frac{F(\gamma_1, \zeta_1)}{4} \right)$$

V. NUMERICAL RESULTS

We assess the performance of the proposed techniques in a mMIMO scenario where both the $\mathcal{S}-\mathcal{R}$ and $\mathcal{R}-\mathcal{D}$ distances are set to $d=300$ m, the signal carrier frequency is $f_c = 2.6$ GHz, and the signal bandwidth is $B=200$ kHz. The path loss for both links is given by $a_i = (\frac{c}{4\pi f_c})^2 d^{-p_e} = -115$ dBm, $i=1, 2$, where $p_e=3$ is the path loss exponent and c is the speed of light. The additive noise at both relay and destination has power spectral density $N_0 = -174$ dBm/Hz, so that the noise terms are given by $I_1 = I_2 = N_0 B = -121$ dBm. Moreover, we assume that the eigenvalues of $\tilde{\mathbf{H}}_i^H \tilde{\mathbf{H}}_i$ follow the Marčenko-Pastur law.

In such conditions and for the ‘‘OPT’’, ‘‘ZF’’, and ‘‘MMSE’’ techniques, Fig. 2 shows the asymptotic transmit power $p_1^{*,\infty}(p_2)$ plotted versus p_2 , for $\psi^\infty=0.5$, $p_1^{\max} = 1$ mW, $\beta = -110$ dB, and $\zeta_1=0.5$. For the sake of comparison, the plot also depicts the asymptotic power profile obtained when perfect CSI is available at the source and \mathcal{S} applies singular value decomposition (SVD) precoding, as described in [7, Formula 35]. Note that, when considering our benchmark (i.e., SVD precoding at the transmitters) no ZF or MMSE filters are considered at the receivers. When both $p_1^{*,\infty}$ and p_2 are positive, \mathcal{R} works in FD mode, whereas $p_1^{*,\infty}=0$ indicates that \mathcal{R} works in half-duplex (HD) mode. When the ‘‘MMSE’’ and ‘‘OPT’’ techniques are employed, \mathcal{R} is allowed to work in FD mode for $p_2 < \omega^{\text{OPT}} \approx 1.17$ mW; this threshold reduces to $p_2 < \omega^{\text{ZF}} \approx 0.545$ mW for the ‘‘ZF’’ technique. Instead, for the ‘‘SVD’’ case, we have $p_1^{*,\infty} > 0$ for $p_2 < \omega^{\text{SVD}} \triangleq \frac{1}{\beta} \left(\frac{\alpha_1(1 - \sqrt{\zeta_1})^2}{\psi^\infty \zeta_1} - I_1 \right) \approx 3.56$ mW. Since $\omega^{\text{SVD}} > \omega^{\text{OPT}} > \omega^{\text{ZF}}$ (the proof follows from the definition of such terms), SVD is the most efficient in exploiting relay FD capabilities, as it allows \mathcal{S} to transmit for larger values of p_2 . However, as mentioned, it requires full CSI at the transmitter. As for the other techniques, while sharing the same threshold ω^{OPT} with ‘‘MMSE’’, ‘‘OPT’’ allows \mathcal{R} to transmit at higher power than ‘‘MMSE’’, thus leading to a higher relay efficiency.

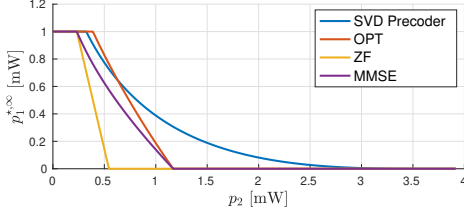


Fig. 2. Asymptotic transmit power profile $p_1^{*,\infty}(p_2)$ vs p_2 for $\beta = -110$ dB, $\psi_\infty = 0.5$, $\zeta_1 = 0.5$, and $p_1^{\max} = 1$ mW.

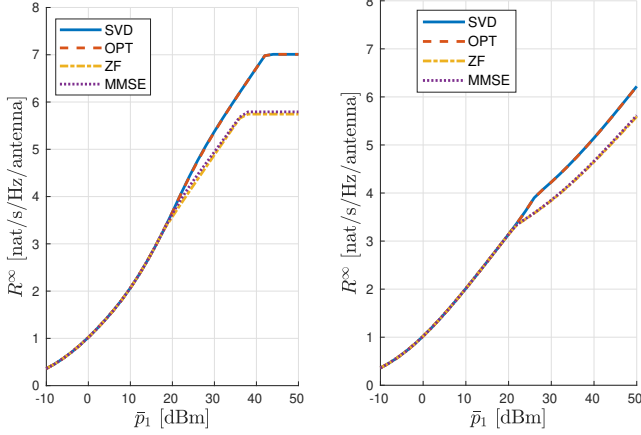


Fig. 3. E2e normalized rate vs \bar{p}_1 , for SVD precoding on the $\mathcal{S} - \mathcal{R}$ link and the analysed techniques with no precoding on the $\mathcal{R} - \mathcal{D}$ one. SVD on the $\mathcal{R} - \mathcal{D}$ link (blue line) is taken as benchmark. $\beta = -125$ dB (left) and $\beta = -110$ dB (right).

Fig. 3 shows the asymptotic normalized rate, R^∞ plotted versus \bar{p}_1 when the analysed techniques with no precoding are used on the $\mathcal{S} - \mathcal{R}$, compared to the case where SVD precoding is employed on the $\mathcal{S} - \mathcal{R}$ link (in which case no OPT, ZF, or MMSE are used at the receiver). Fig. 4, instead, presents the system performance when the same technique is applied to both links (again, SVD-SVD, with no OPT, ZF, or MMSE at the receiver, is used as benchmark). For both figures, we set $p_1^{\max} = \bar{p}_1 + 3$ dB, $\bar{p}_2 = 20$ dBm, $p_2^{\max} = 23$ dBm, $\zeta_1 = \zeta_2 = 0.8$, and $\zeta_r = 1$. Also, the left plots in both figures refer to a relay self-interference attenuation $\beta = -125$ dB, while the right plots correspond to $\beta = -110$ dB. Rate R^∞ is computed solving (13), by discretizing density $g(p_2)$ as shown in [7]. Also, in Fig. 4 the numerical values, R/n_1 , are obtained by solving the problem as in (8), for $n_1 = 64$. In the considered scenario, we notice that “OPT” matches the performance of “SVD”, while not requiring CSI knowledge at the transmitter. Further, “MMSE” and “ZF” behave very similarly and, although suboptimal, they entail only a moderate performance degradation with respect to “OPT”. In particular, Fig. 3 shows that when “SVD” is applied to the $\mathcal{S} - \mathcal{R}$ link, the choice of the technique on the $\mathcal{R} - \mathcal{D}$ link does not have a significant impact, especially for low values of \bar{p}_1 . Also, the performance is very sensitive to the self-interference attenuation: when β changes from -110 dB to -125 dB, R^∞ increases by about 1 nat/s/Hz per transmit antenna at $\bar{p}_1 = 30$ dBm, which highlights the importance of self-interference attenuation at the relay. Finally, we underline the excellent match between asymptotic and numerical results.

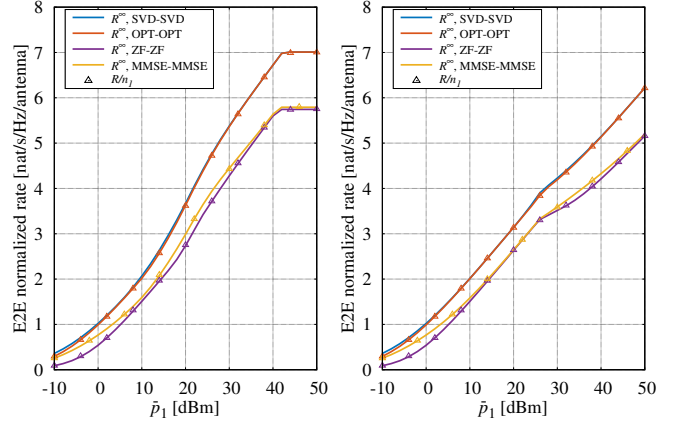


Fig. 4. Asymptotic and numerical e2e normalized rate vs \bar{p}_1 , for the analyzed techniques with no precoding on either links, and the SVD-SVD benchmark (blue line). $n_1 = 64$, $\beta = -125$ dB (left) and $\beta = -110$ dB (right).

VI. CONCLUSIONS

We addressed massive MIMO full-duplex relay networks working in decode-and-forward mode, where CSI at any of the transmitters is unavailable. We studied the system performance when precoding is implemented at neither the source nor the relay, or it can be performed at the source only. To this end, we considered the transmit power at the source to depend on that at the relay, and formulate a problem that aims at maximizing the end-to-end network rate. Then, by letting the number of antennas grow large, we obtain closed-form expressions for the nodes transmit power and the system data rate. Our results show that with no precoding at the relay, or even at neither the transmitting nodes, the data rate closely matches the values achieved with SVD precoding when the optimum receiver is used, and no substantial degradation is observed in the case of ZF or MMSE receivers.

REFERENCES

- [1] A.-S. Bana, E. de Carvalho, B. Soret, T. Abrão, J. C. Marinello, E. G. Larsson, and P. Popovski, “Massive MIMO for Internet of Things (IoT) connectivity,” *Physical Comm.*, vol. 37, p. 100859, 2019.
- [2] E. Becirovic, “On massive MIMO for massive machine-type communications,” Ph.D. dissertation, Linköping University, 2020.
- [3] X. Wu, X. Yang, S. Ma, B. Zhou, and G. Yang, “Hybrid channel estimation for UPA-assisted millimeter-wave massive MIMO IoT systems,” *IEEE Internet of Things J.*, pp. 1–1, 2021.
- [4] Y. Dai and X. Dong, “Power allocation for multi-pair massive MIMO two-way AF relaying with linear processing,” *IEEE Trans. on Wireless Comm.*, vol. 15, no. 9, pp. 5932–5946, 2016.
- [5] Z. Peng, X. Chen, W. Xu, C. Pan, L.-C. Wang, and L. Hanzo, “Analysis and optimization of massive access to the iot relying on multi-pair two-way massive MIMO relay systems,” *IEEE Trans. on Comm.*, vol. 69, no. 7, pp. 4585–4598, 2021.
- [6] C. D. Ho, H. Q. Ngo, and M. Matthaiou, “Transmission schemes and power allocation for multiuser massive MIMO relaying,” *IEEE Trans. on Veh. Tech.*, 2021.
- [7] A. Nordio and C. F. Chiasserini, “MIMO full-duplex networks with limited knowledge of the relay state,” *IEEE Trans. on Wireless Comm.*, vol. 20, no. 4, pp. 2516–2529, 2021.
- [8] S. Li, M. Zhou, J. Wu, L. Song, Y. Li, and H. Li, “On the performance of X-duplex relaying,” *IEEE Trans. on Wir. Comm.*, vol. 16, no. 3, pp. 1868–1880, March 2017.
- [9] A. Behboodi, A. Chaaban, R. Mathar, and M. Alouini, “On full duplex gaussian relay channels with self-interference,” in *IEEE ISIT*, July 2016, pp. 1864–1868.